Theoretical Study on the Correlation between the Nature of Atomic Li Intercalation and Electrochemical Reactivity in TiS_2 and TiO_2

Yang-Soo Kim,[†] Hee-Jin Kim,[†] Young-A. Jeon,[‡] and Yong-Mook Kang*[,§]

Sunchon Branch, Korea Basic Science Institute, 315 Maegok, Sunchon, Republic of Korea, Department of Materials Science and Engineering, Korea Advanced Institute of Science and Technology, Gusung-dong, Yusung-gu, Daejeon, 305-701, Republic of Korea, and Division of Advanced Materials Engineering, Kongju National University, 275 Budae-dong, Cheonan, Chungnam, Republic of Korea

Received: September 23, 2008; Revised Manuscript Received: December 4, 2008

The electronic structures of $LiTiS_2$ and $LiTiO_2$ (having α-$NaFeO_2$ structure) have been investigated using discrete variational Xα molecular orbital methods. The α-$NaFeO_2$ structure is the equilibrium structure for $LiCoO_2$, which is widely used as a commercial cathode material for lithium secondary batteries. This study especially focused on the charge state of Li ions and the magnitude of covalency around Li ions. When the average voltage of lithium intercalation was calculated using pseudopotential methods, the average intercalation voltage of $LiTiO_2$ (2.076 V) was higher than that of $LiTiS_2$ (1.958 V). This can be explained by the differences in Mulliken charge of lithium and the bond overlap population between the intercalated Li ions and anion in $LiTiO_2$ as well as $LiTiS_2$. The Mulliken charge, which is the ionicity of Li atom, was approximately 0.12 in $LiTiS_2$, and the bond overlap population (BOP) indicating the covalency between Ti and S was about 0.339. When compared with the BOP (0.6) of C−H, which is one of the most famous example of covalent bonding, the intercalated Li ions in $LiTiS_2$ tend to form a quite strong covalent bond with the host material. In contrast, the Mulliken charge of lithium was about 0.79, which means that Li is fully ionized and the BOP, the covalency between Ti and O, was 0.181 in $LiTiO_2$. Because of the high ionicity of Li and the weak covalency between Ti and the nearest anion, $LiTiO_2$ has a higher intercalation voltage than $LiTiS_2$.

Introduction

The appropriate cathode materials for lithium secondary batteries have been investigated due to the exponential growth in energy storage equipment of distributed power as well as portable electronic devices such as cellular phones and laptop computers. As a result, a number of materials which are capable of the insertion or extraction of Li ion have been introduced. In the 1970s, transition-metal chalcogenides, e.g., TiS_2 and MoS_2, attracted major attention as the cathode materials. TiS_2 has a layered structure. During discharge, the Li ion inserts into the van der Waals gap between the sulfide layers and the charge balance is maintained by a reduction of the Ti^{4+} ions to Ti^{3+}. During charge, exactly the reverse process involving the extraction of Li ion from the van der Waals gap and an oxidation of Ti^{3+} to Ti^{4+} occurs. During the charge/discharge process, its layered structure is maintained, resulting in a good reversibility. However, in the 1980s, Mizushima et al. reported a $LiCoO_2$ material[1] whose voltage is as high as approximately 4 V against metallic lithium, while the voltages in most of transition-metal chalcogenides are approximately 2 V. Thereafter, many kinds of research on the 3d transition-metal oxides for the electrode materials have been performed.[2−4] The reason why transition-metal oxides show higher voltage compared to chalcogenides including transition metals is not clear even though there has been a previous report to analyze the chemical bonding of $LiTiX_2$ (X = S, Se, and Te).[5] Actually, we need more fundamental information on the correlation between electronic states and electrochemical properties of materials as guiding principles for designing more enhanced electrode materials.

TABLE 1: Calculated Lattice Parameters and Interatomic Distances That Gave the Lowest Energy for TiS_2, TiO_2, $LiTiS_2$, and $LiTiO_2$

	space group	lattice constant (*i*), Å		interatomic distance (*i*), Å	
		a	*c*	$d_{Ti-O(S)}$	$d_{Li-O(S)}$
$LiTiS_2$	$P\bar{3}m1$ (164)	3.433	6.177	2.467	2.559
TiS_2	$P\bar{3}m1$ (164)	3.378	5.968	2.424	
$LiTiO_2$	$R\bar{3}m$ (166)	2.893	14.752	2.053	2.095
TiO_2	$R\bar{3}m$ (166)	2.966	13.689	1.977	

Theoretical calculations of $LiTiS_2$ were first attempted by McCanny using a semiempirical tight-binding method.[6] He insisted that the change in electronic states of TiS_2 during Li ion insertion can be explained by a simple rigid-band filling. In his results, Li donates an electron to the host TiS_2 in order to make the valence state of Li ion +1 without changing the band structure. A more reliable calculation using the linearized augmented plane-wave (LAPW) method was reported by Umrigar et al.[7] They described in detail the change of electronic density of states (DOS) associated with the intercalation of Li ion. Of course, the band structure cannot be rigorously rigid. Their calculation could not explain why Li is not completely ionized, differing from the assumption of the McCanny model. Furthermore, they did not figure out the change of chemical bonding during Li ion insertion.

Even though the existence of $LiTiO_2$ has been recognized theoretically[8−11] and extrapolated experimentally,[11−13] the feasibility of $LiTiO_2$ (or the metastable cubic $Li_2Ti_2O_4$ which could be converted to the rock salt $LiTiO_2$ upon heating 600 °C) was

* Corresponding author. Tel.: +82-16-257-9051. Fax: +82-41-568-5776. E-mail: dake@kaist.ac.kr or dake1234@kongju.ac.kr.
† Korea Basic Science Institute.
‡ Korea Advanced Institute of Science and Technology.
§ Kongju National University.

10.1021/jp808426t CCC: $40.75
Published on Web 01/12/2009

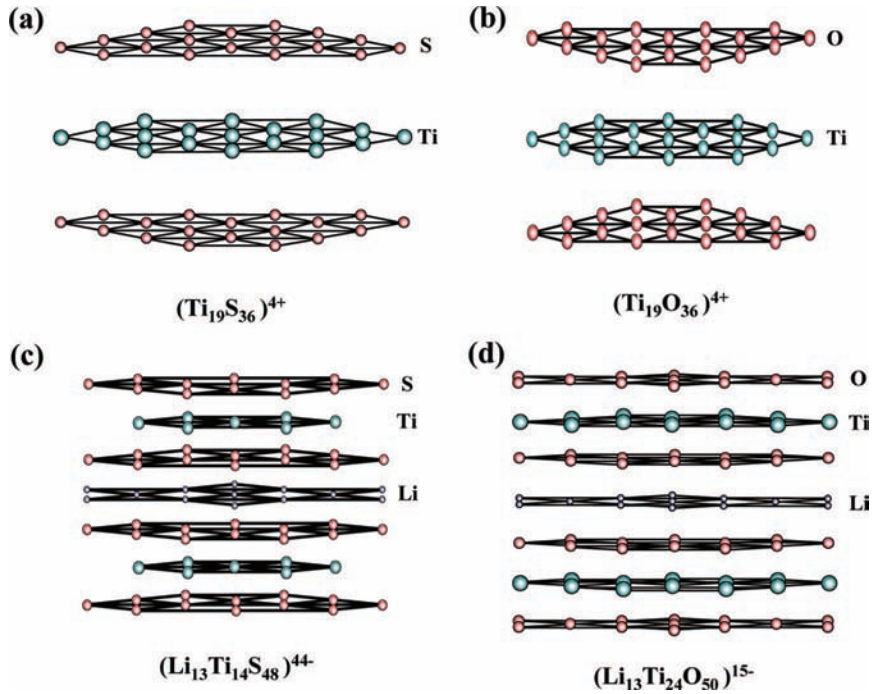

Figure 1. Cluster models for calculating the electronic structures of TiS_2, TiO_2, $LiTiS_2$, and $LiTiO_2$: (a) $(Ti_{19}S_{36})^{4+}$ for TiS_2, (b) $(Ti_{19}O_{36})^{4+}$ for TiO_2, (c) $(Li_{13}Ti_{14}S_{48})^{44-}$ for $LiTiS_2$, and (d) $(Li_{13}Ti_{24}O_{50})^{15-}$ for $LiTiO_2$.

confined to a few cases in which the chemical synthesis is utilized.[14,15] In this paper, we focused on the systematic understanding of the chemical bonding of Li inserted into TiS_2 and TiO_2 using first-principles calculations. It is because the average potential depends on the chemical nature of the nearest neighboring anion, which affects the strength of the transition metal−anion bonds. Hence, the purpose of this study is to simulate the electronic structure and chemical bonding of transition-metal oxides and chalcogenides, which can determine the average voltage associated with the electrochemical reduction of Ti^{4+} to Ti^{3+}.

Experimental Section

Two kinds of first-principles calculations were combined in order to evaluate the average voltage and understand the electronic mechanism determining the voltage. First-principles total energy calculations using the generalized gradient approximation (GGA) to density functional theory as implemented in the Vienna Ab Initio Simulation Package (VASP), which enables geometry optimization, was allowed for a quantitative discussion of the voltage. Ultrasoft pseudopotentials were used with a plane-wave cutoff of 400 eV. Because the detailed magnetic structure in $LiTiS_2$ and $LiTiO_2$ has not been known, we assumed a ferromagnetic spin ordering for simplicity. Table 1 shows the calculated lattice parameters and interatomic distances that gave the lowest energy for these compounds.

The electronic structures were analyzed using first-principles molecular orbital calculations by the DV-Xα method using model cluster in order to discuss the electronic mechanism determining the voltage.[16,17] We chose $(Li_{13}Ti_{14}S_{48})^{44-}$, $(Li_{13}Ti_{24}O_{50})^{15-}$, $(Ti_{19}S_{36})^{4+}$, and $(Ti_{19}O_{36})^{4+}$ as the model clusters for $LiTiS_2$, $LiTiO_2$, TiS_2, and TiO_2, respectively (Figure 1) Lattice parameters were adopted from the theoretical data obtained by VASP. Model clusters were embedded in point charges located at the external atomic sites to produce an effective Madelung potential.

Results and Discussion

In order to discuss the valence electronic state and chemical bonding of TiS_2, we made calculations using a cluster model ($(Ti_{19}S_{36})^{4+}$) mentioned in the computational procedure. Figure 2a shows the density of states (DOS) of TiS_2 obtained by this calculation. The energy scale was shifted to make the Fermi level (E_F) zero. In Figure 2a, the partial density of states (PDOS) for each atomic orbital is also plotted. The valence state is composed of S 3s band at −10∼−15 eV and S 3p band at 0∼−5 eV. However, these states include considerably large amounts of Ti atomic orbitals as the components. Above the E_F, the Ti 3d band is located. This band consists of two peaks (c_1 and c_2), which can be ascribed to t_{2g} and e_g type bands, respectively. Because all transition-metal ions are located at the octahedral sites in a cubic close-packed (CCP) oxygen sublattice, the 3d bands of transition-metal ions are split into t_{2g}-like and e_g-like bands. The Ti 3d bands also involve a large amount of S 3p components. The characteristic feature of the S 3p valence band located at 0∼−5 eV is the presence of three peaks labeled as v_1, v_2, and v_3 in it. As shown in the next paragraph, these states originate from the overlapping of S 3p−Ti 3d orbitals, which bring about very strong covalent interaction between S and Ti atoms.

Even if the valence state is mainly constructed by S 3s band and S 3p band, this band also contains Ti 3d and 4sp orbitals in notable mounts, contributing to the strong Ti−S covalent bonding. As a result, the origins of three peaks in the S 3p band are as follows: v_1, Ti 4sp−S 3p bonding; v_2, Ti 3d−S 3p bonding; v_3, S 3p nonbonding. For further understanding of the covalency, the density of states is shown in Figure 2b together with the energy distribution of the overlap population. With regard to the bond overlap population, a positive value indicates the presence of the bonding type interaction, whereas a negative value reflects the presence of the antibonding type interaction operating between electron orbitals. For Ti−S bonding, no antibonding contribution can be found below E_F. Therefore, as explained from the above discussion, we can say that the strong covalent bonding exists between Ti and S. In the case of Ti−Ti

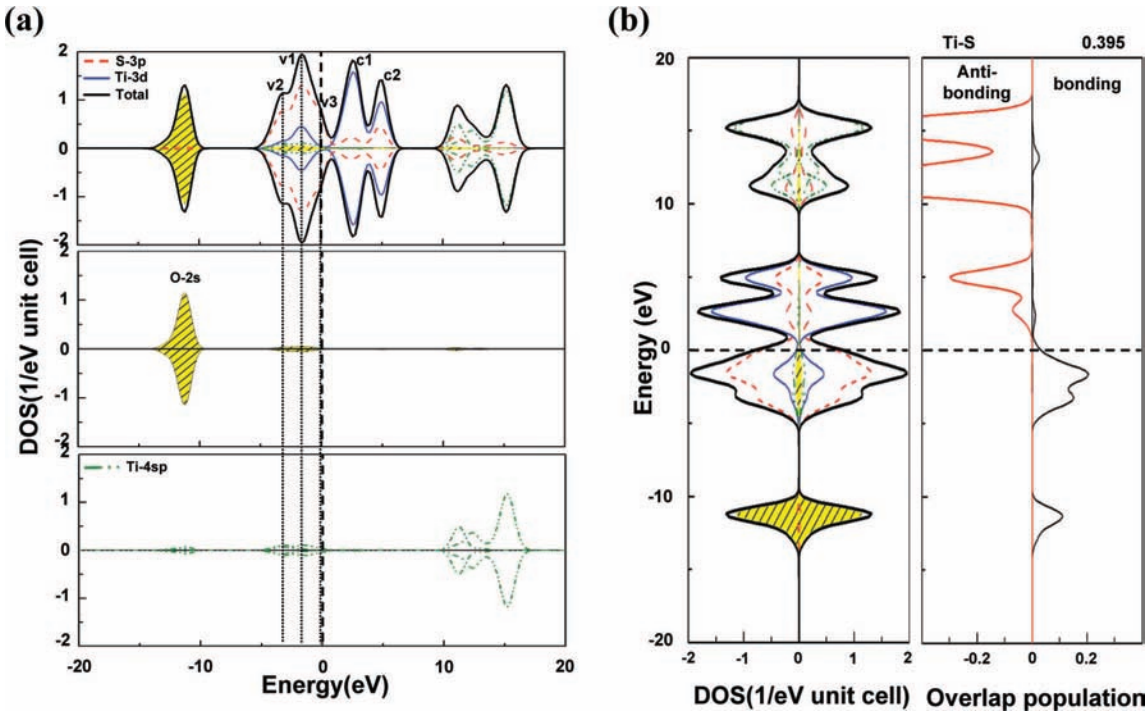

Figure 2. (a) Total density of states for TiS_2 and partial density of states for each atomic orbital. The energy scale was shifted to make the E_F zero. (b) Bond overlap population diagram between Ti and S in TiS_2.

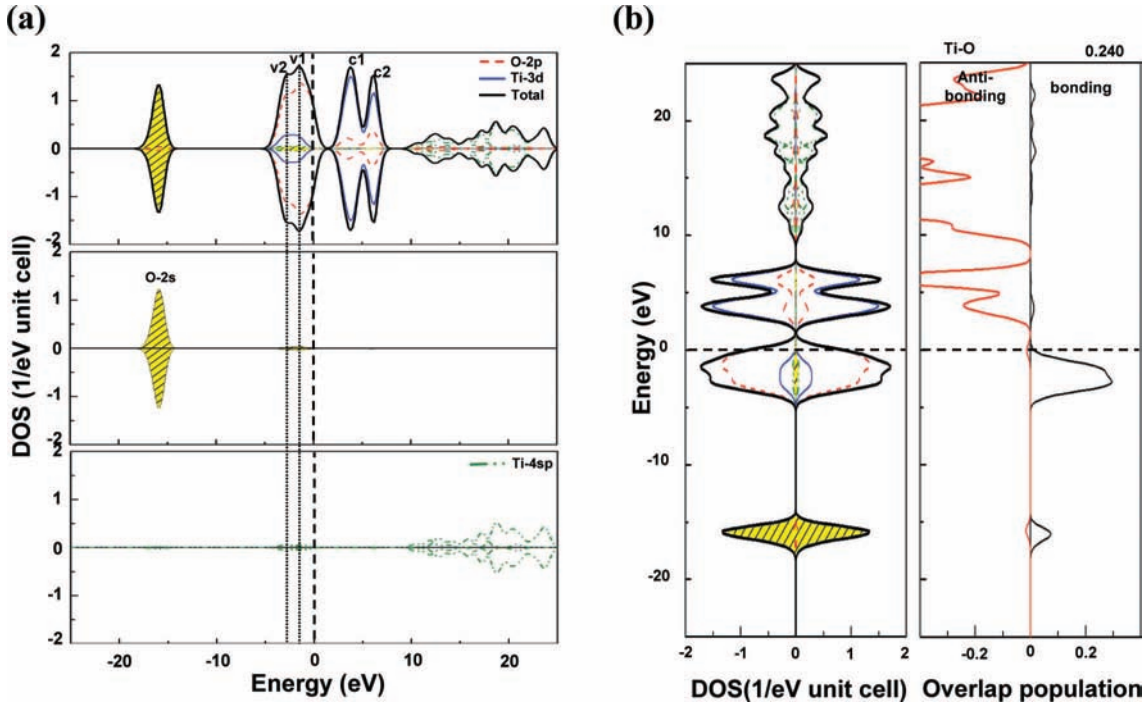

Figure 3. (a) Total density of states for TiO_2 and partial density of states for each atomic orbital. The energy scale was shifted to make the E_F zero. (b) Bond overlap population diagram between Ti and O in TiO_2.

bonding, its bond overlap population is very small except for the high-energy region of its conduction band.

Figure 3a shows the total and partial density of states of TiO_2. O 2s and O 2p bands primarily construct the valence state of TiO_2. However, the O 2p band notably includes Ti 3d orbitals, indicating the evolution of Ti−O covalent bonding. The Ti 3d band is intensively located around the E_F just like in TiS_2. A band mainly composed of Ti−4sp orbitals appears from approximately 12 eV above the Fermi energy. In order to confirm the Ti−O covalency, its bond overlap population is shown in Figure 3b. Because the significant antibonding Ti−O interactions exist around the E_F unlike Ti−S bonding, the bond overlap population of Ti−O is relatively small compared with that of Ti−S, implying that TiO_2 has a small covalency.

When Li is introduced into the Van der Waals gap of TiS_2, Li 2sp PDOS apparently overlaps with S 3s and 3p bands, inducing the strong Li−S covalency which prevents Li from being completely ionized. Figure 4a shows that the d states of $LiTiS_2$ are scarcely affected by Li intercalation and Li electron density increases only upon filling the bands of the host material. However,

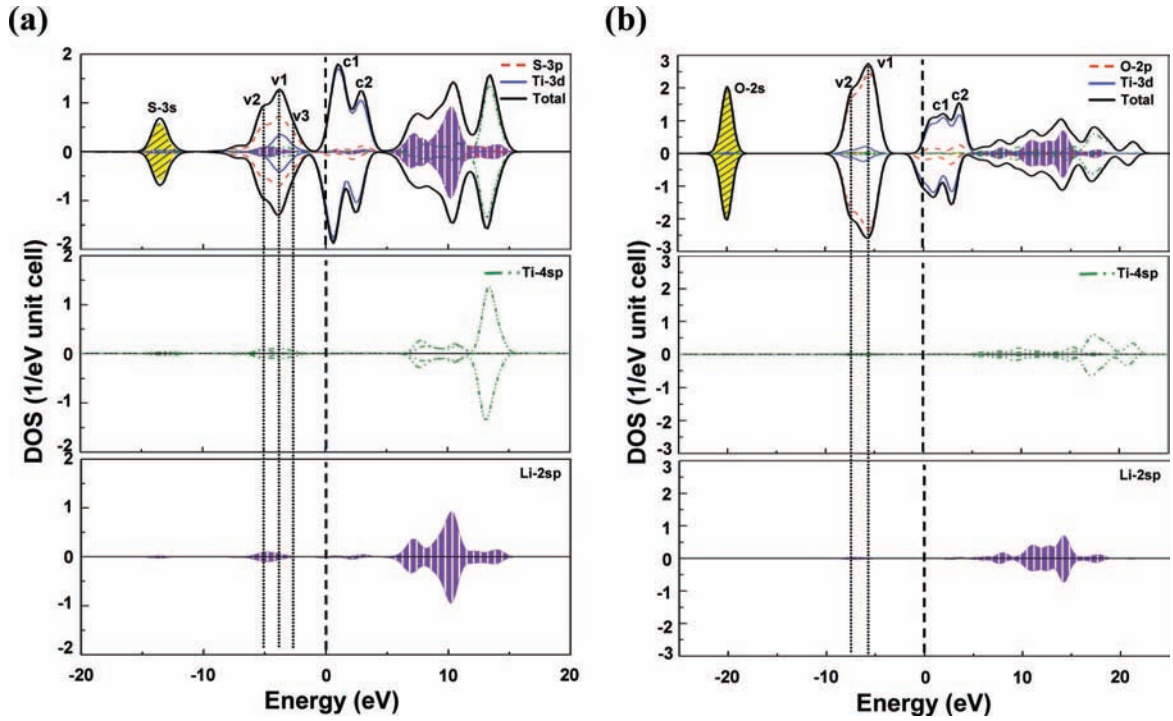

Figure 4. (a) Total density of states for $LiTiS_2$ and its partial density of states for each atomic orbital. (b) Total density of states for $LiTiO_2$ and its partial density of states for each atomic orbital.

TABLE 2: Bond Overlap Population, Net Charge, and Average Voltage (vs. Li/Li$^+$) of TiS_2, TiO_2, $LiTiS_2$, and $LiTiO_2$ Obtained from Mulliken's Population Analysis

	bond overlap population			
	Ti−S(O)	Li−S(O)	Li net charge	average voltage, V (vs Li/Li$^+$)
$LiTiS_2$	0.339	0.174	0.12	1.958
TiS_2	0.395			1.958
$LiTiO_2$	0.181	0.018	0.79	2.076
TiO_2	0.24			2.076

it is certain that the intercalation of Li into TiO_2 induces some significant rearrangement of bands. As shown in Figure 4b, the almost filled band located between 0 and −8 eV is mainly composed of O 2p orbitals, and the partially filled band located around the E_F is constructed by Ti 3d orbitals. On the other hand, the unoccupied band above 10 eV is made up of Li 2sp and Ti 4sp orbitals. Li 2sp states make little contribution to the valence band, suggesting that Li is nearly ionized in $LiTiO_2$. Contrarily, significant amounts of Ti 3d, 4s, and 4p orbitals are found in the O 2p band. This phenomenon can imply that there are strong covalent interactions between Ti and O. This can be attributed to the fact that Li in $LiTiO_2$ features a completely ionic character and makes little covalent interaction with the surrounding atoms. For evaluating the ionicity of Li in $LiTiS_2$ and $LiTiO_2$, Mulliken's population analysis has been conducted. Bond overlap population, net charge, and average voltage obtained from this calculation are summarized in Table 2.

As shown here, the net charges of Li for $LiTiS_2$ and $LiTiO_2$ are 0.12 and 0.79, respectively. Because the formal charge of Li is +1, a large deviation from this charge implies that the Li is not purely ionic but partially covalent. These values indicated that Li intercalates into TiS_2 with little electron donation to the host compared to $LiTiO_2$. The reason why Li in $LiTiS_2$ features higher covalency may be due to the presence of Li 2sp orbitals in the valence band, followed by the augmented bond overlap population of Li−S (Figure 4a) The bond overlap population of Ti−S decreases from 0.395 to 0.339 after Li intercalation. The diminution of bond overlap population for Ti−S, associated with the Li intercalation, can be ascribed to two phenomena: the coexistence of Li−S bonding and Ti−S bonding in the S 3sp bands and a little longer Ti−S bond distance in $LiTiS_2$ than in TiS_2 as indicated in Table 1.[5] Meanwhile, $LiTiO_2$ has a significant covalent bonding between Ti and O (0.181), and much smaller covalency in Li−O bonds (0.018). As indicated by the net charge, the oxidation state of Li in $LiTiO_2$ is nearly +1, showing the nearly perfect ionicity of Li in the host material. The decrease of bond overlap population after Li intercalation into TiO_2 may result from the injection of an electron to the Ti 3d band, in which the Ti−O bonding features a remarkable antibonding character. This means that the nature of the Ti−O bond is hardly affected by the presence of intercalated Li. So, we can say that Li is almost ionized for Li transition-metal oxides. Actually, the ionicity of Li is a very important factor in determining the open circuit voltage (OCV) for Li-intercalating oxides or chalcogenides.

In order to estimate the average voltage of $LiTiS_2$ or $LiTiO_2$, the following equation[18] was used and the results are shown in Table 2.

$$V_{ave} = \frac{E_{tot}[LiTiS(O)_2] - E_{tot}[TiS(O)_2] - E_{tot}[Li]}{e}$$

where $E_{tot}[]$ is the total energy per formula unit and e is the elementary electric charge. As a result of calculation, we observed that the average voltage of $LiTiO_2/TiO_2$ (2.076 V vs Li/Li$^+$) is higher than that of $LiTiS_2/TiS_2$ (1.958 V vs Li/Li$^+$). Herein, it should be noted that the higher the given redox reaction energy, the lower the average voltage for this redox reaction. Because the redox reaction energy of Li-intercalating materials is proportional to the covalency strength between transition metal and the surrounding anions, a low average voltage tends to be involved with a strong covalent bonding between transition metal and the surrounding anions.[19] As a

representative example for this phenomenon, the following research can be suggested. J. B. Goodenough et al. have shown that the electrochemical potential of materials utilizing the Fe^{3+}/Fe^{2+} redox couple can be tuned by anionic substitution.[20,21] When the Fe^{3+}/Fe^{2+} couple acted as the redox center, the electrochemical potential of $Fe_2(SO_4)_3$, $LiFe_2(SO_4)_2(PO_4)$, and $Li_3Fe_2(PO_4)_3$ corresponded to 3.6, 3.4, and 2.8 V (vs Li/Li^+), respectively. It was because the $Fe-PO_4$ bonding features more covalency than the $Fe-SO_4$ bonding. As previously discussed, nonionicity of Li in $LiTiS_2$ leads to the augmentation of covalency between Ti and S, while the extreme ionicity of Li in $LiTiO_2$ is followed by the disappearing covalency between Ti and O. As a consequence, Ti−S bonding would show stronger covalent character than Ti−O bonding, which results in an increased redox reaction energy of Ti^{4+}/Ti^{3+}. So, it seems to be natural that $LiTiO_2$ has a higher average operating voltage than $LiTiS_2$.

Conclusion

The electronic structure and chemical bonding of the Li-intercalated TiX_2 (X = S and O) have been studied by two kinds of first-principles calculations, molecular orbital (MO) calculations by the DV-Xα method and the ab initio total energy and molecular dynamics program VASP (Vienna Ab-inition Simulation Package). Mulliken's population analysis has been thoroughly conducted to examine the net charge as well as the magnitude of covalency. We found that apparently the Mulliken charges of Li in $LiTiX_2$ (X = S and O) and the bond overlap population of Li−X are different depending on the X species. These chemical natures affect the average intercalation voltage: $LiTiS_2$ shows lower average voltage compared to $LiTiO_2$ owing to the superior covalency of Ti−S bonding to Ti−O bonding. In this present study, we have clarified the notable characteristics in the electronic state and chemical bonding of titanium disulfides, which are clearly different from those of the titanium dioxides. Furthermore, we have found that the electronic state and chemical bonding of interacted Li ion in the titanium disulfides is very different from those in the oxides. The information on the electronic characteristics of these materials can be helpful for their application to energy storage devices like Li ion secondary batteries.

Acknowledgment. This work was supported by the Ministry of Education ("Brain Korea 21") and the Ministry of Science and Technology. This work was also supported by the Korea Science and Engineering Foundation (KOSEF) grant funded by the Korea government (MEST) (R01-2008-000-11061-0) and the Korea Research Foundation grant funded by the Korean Government (MOEHRD, Basic Research Promotion Fund) (KRF-2008-331-D00247).

References and Notes

(1) Mizushima, K.; Jones, P. C.; Wiseman, P. J.; Goodenough, J. B. *Mater. Res. Bull.* **1980**, *15*, 783.
(2) Ohzuku, T.; Ueda, A. *Solid State Ionics* **1994**, *69*, 201.
(3) Jeon, Y. A.; Kim, S. K.; Kim, Y. S.; Won, D. H.; Kim, B. I.; No, K. S. *J. Electroceram.* **2006**, *17*, 667.
(4) Jeon, Y. A.; Kim, Y. S.; Kim, S. K.; No, K. S. *Solid State Ionics* **2006**, *117*, 2661.
(5) Kim, Y. S.; Koyama, Y.; Tanaka, I.; Adachi, H. *Jpn. J. Appl. Phys.* **1998**, *37*, 6440.
(6) McCannby, J. V. *J. Phys. C* **1979**, *12*, 3263.
(7) Umrigar, C.; Ellis, D. E.; Wang, D. S.; Krakauer, H.; Posternak, M. *Phys. Rev. B* **1982**, *26*, 4935.
(8) Mackrodt, W. C. *J. Solid State Chem.* **1999**, *142*, 428.
(9) Benco, L.; Barras, J. L.; Daul, C. A.; Deiss, E. *Inorg. Chem.* **1999**, *38*, 20.
(10) Koudriachova, M. V.; Harrison, V. M.; de Leeuw, S. W. *Phys. Rev. Lett.* **2001**, *86*, 1275.
(11) Lecerf, A. *Ann. Chim.* **1962**, *7*, 519.
(12) Shirance, G.; Pickarty, S. J.; Newnham, R. *J. Phys. Chem. Solids* **1960**, *12*, 155.
(13) Koudriachova, M. V.; de Leeuw, S.; Harrison, W. V. M. *Chem. Phys. Lett.* **2003**, *371*, 150.
(14) Murphy, D. W.; Greenblatt, M.; Zahurak, S. M.; Cava, R. J.; Waszczak, J. V.; Hull, G. W.; Hutton, R. S. *Rev. Chim. Miner.* **1982**, *19*, 441.
(15) Murphy, D. W.; Cava, R. J.; Zahurak, S. M.; Santoro, A. *Solid State Ionics* **1983**, *9−10*, 413.
(16) Ellis, D.; Adachi, E. H.; Averill, F W. *Surf. Sci.* **1976**, *58*, 491.
(17) Adachi, H.; Tsukada, M.; Satoko, C. *J. Phys. Soc. Jpn.* **1978**, *45*, 875.
(18) Aydinal, M. K.; Kohan, A. F.; Ceder, G.; Cho, K.; Joannopoulo, J. *Phys. Rev. B* **1997**, *56* (3), 1354.
(19) Goodenough, J. B. *General Concepts in Lithium Ion Batteries: Fundamentals and Performance*; Wiley-VCM: Weinheim, 1998.
(20) Masquelier, C.; Padhi, A. K.; Nanjundaswamy, K. S.; Goodenough, J. B. *J. Solid State Chem.* **1998**, *135*, 228.
(21) Padhi, A. K.; Manivannan, V.; Goodenough, J. B. *J. Electrochem. Soc.* **1998**, *145* (5), 1518.

JP808426T